

Optical spectroscopy study on the charge  
dynamics of URu<sub>2</sub>Si<sub>2</sub>

Nan-Lin Wang

Institute of Physics  
Chinese Academy of Sciences

- **Some basics about optical spectroscopy**

Optical constants, Kramers-Kronig transformation, inter- and intra-band transitions

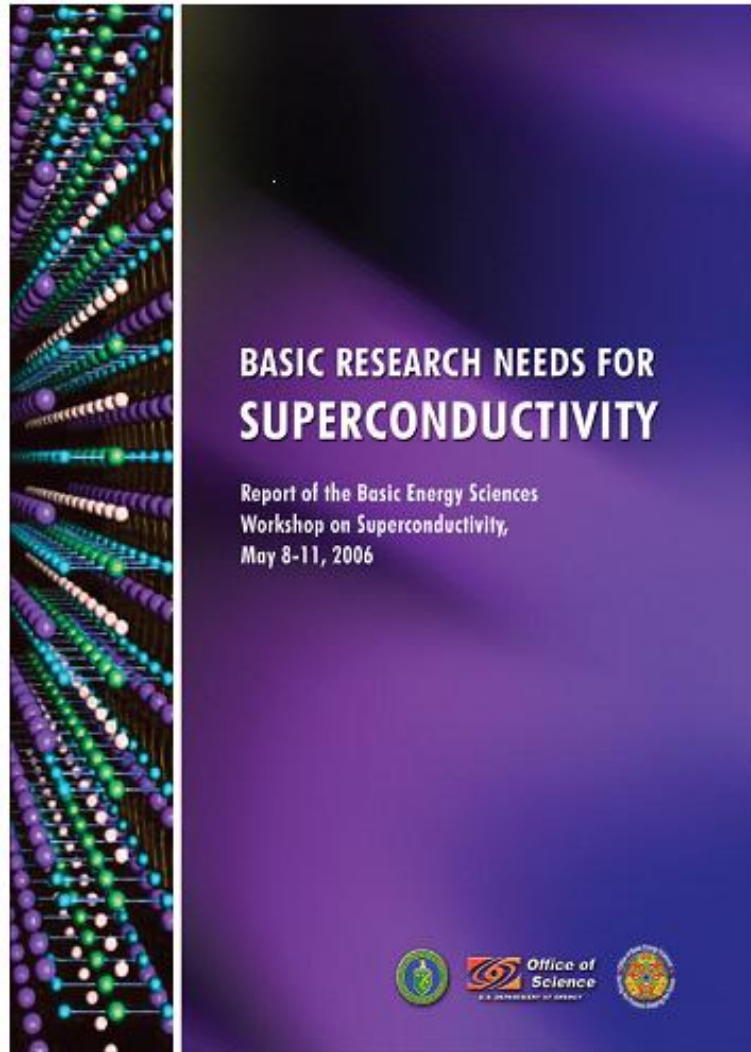
- **Example of application:  
URu<sub>2</sub>Si<sub>2</sub>**

Collaborators:

W. T. Guo, Z. G. Chen (optical measurements)

G. Luke (single crystals)

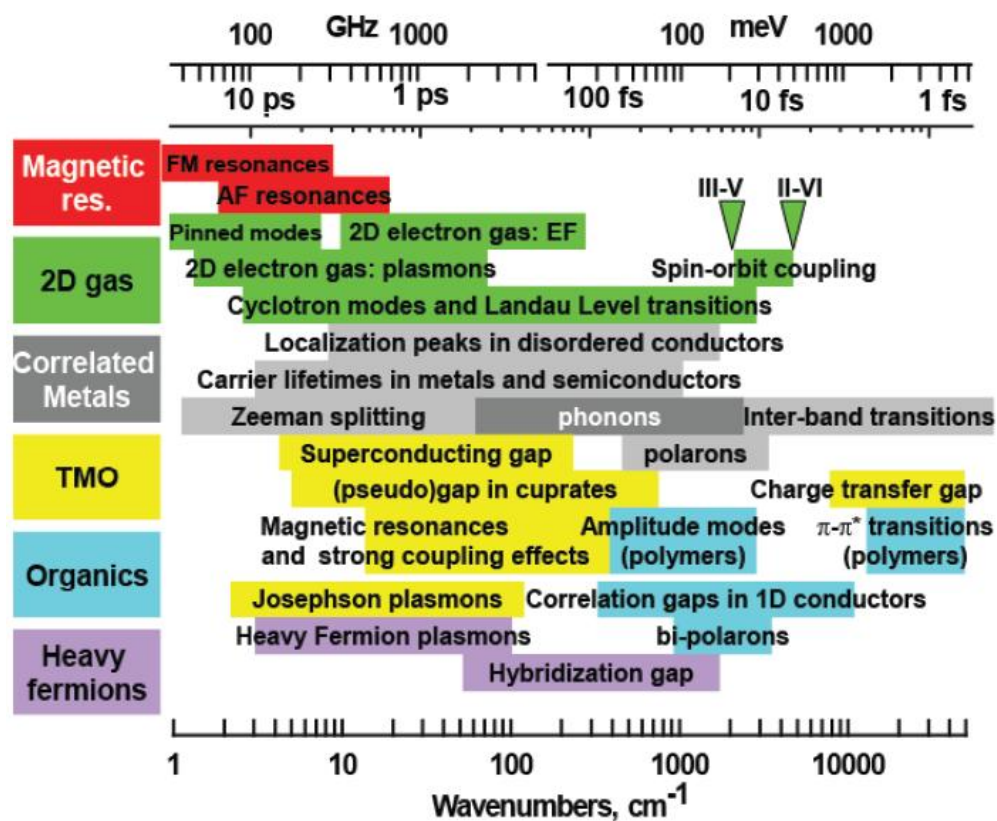
## Some basics about optical spectroscopy technique



### ***Emerging Experimental Techniques and Opportunities***

- *Angle-Resolved Photoemission Spectroscopy (ARPES)*. Wavelike quantum states of the electrons are defined in momentum space ( $k$ -space). ARPES allows direct determination of the complete momentum-space electronic structure,  $A(k, E)$ , with remarkable energy and momentum resolution.
- *Spectroscopic Imaging-Scanning Tunneling Microscopy (SI-STM)*. This is the complementary technique to ARPES that allows mapping of the energy-resolved quantum states in real space ( $r$ -space) with atomic resolution and yet over large sample areas.
- *Microwave/terahertz/infrared/optical spectroscopies*. These probe the electronic excitations and charge dynamics in both the frequency and time domains. This information is the key to understanding the dynamical interactions of the electrons.
- *Resonant elastic and inelastic x-ray spectroscopy*. Resonant elastic and inelastic x-ray scattering can now reveal spin and charge density waves and superlattices with tiny modulation amplitudes. This information is critically important for understanding spatially periodic electronic states of matter.
- *Neutron Scattering (NS)*. High-intensity NS for example, from the Spallation Neutron Source will allow precision measurements of both magnetic ground states and the complete spectrum of magnetic excitations in high-temperature and exotic superconductors.
- *NMR/NQR/ $\mu$ SR*. NMR measures spin dynamics, NQR measures the charge heterogeneity and dynamics, and  $\mu$ SR measures nanoscale variation in local magnetic field strength. These are essentially local spin/charge probes, but without imaging capabilities.

# Optical spectroscopy of solids



Absorption mechanisms associated with various excitations and collective modes in solids  $\rightarrow$  *optical experiments*

(i) measure both  $R(\omega)$  and  $T(\omega)$  for transparent materials

(ii) measure  $R(\omega)$  or  $T(\omega)$ , then use Kramers-Kronig (KK) transformation

(iii) spectroscopic ellipsometry

(iv) THz time-domain spectroscopy...

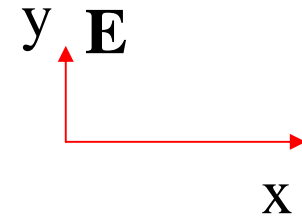
$\rightarrow$  *complex optical constants*

D. N. Basov, Richard D. Averitt, Dirk van der Marel, Martin Dressel, Kristjan Haule  
Rev. Mod. Phys., 2011

Units:  $1 \text{ eV} = 8065 \text{ cm}^{-1} = 11400 \text{ K}$   
 $1.24 \text{ eV} = 10000 \text{ cm}^{-1}$

# Optical constants

Consider an electromagnetic wave in a medium



$$E_y = E_0 e^{i(qx - \omega t)} = E_0 e^{i\omega(x/v - t)} = E_0 e^{i\omega\left(\frac{nx}{c} - t\right)}$$

where  $v \equiv \omega/q = c/n(\omega)$ ,  $n(\omega)$ : refractive index

If there exists absorption,

$$E_y = E_0 e^{-\frac{\omega K x}{c}} e^{i\omega\left(\frac{nx}{c} - t\right)}$$

K: attenuation factor

Intensity

$$I \propto E_y^2 = E_0^2 e^{-\frac{2\omega K x}{c}}$$

Introducing a complex refractive index:

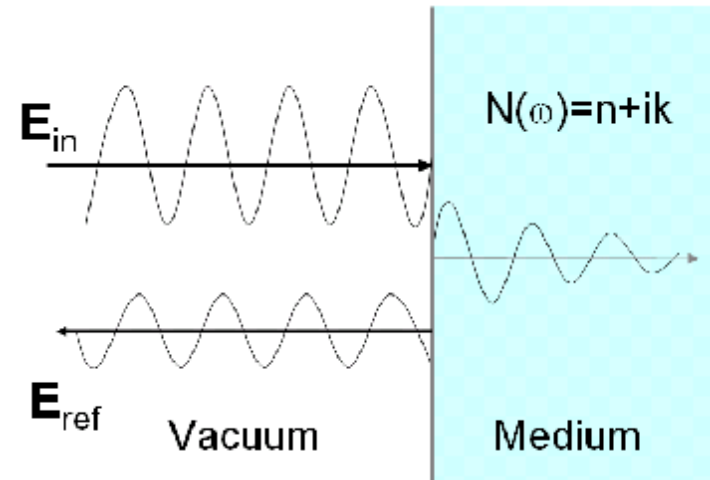
$$N(\omega) \equiv n(\omega) + iK(\omega)$$

$$E_y = E_0 e^{i\omega\left(\frac{N(\omega)x}{c} - t\right)}$$

# Reflectivity

$$\frac{E_{ref}}{E_{in}} \equiv r = r(\omega)e^{iq(\omega)}$$

$$= \frac{n + iK - 1}{n + iK + 1} = \sqrt{\frac{(n-1)^2 + K^2}{(n+1)^2 + K^2}} e^{iq(\omega)}$$



$$R \propto |E_{ref} / E_{in}|^2 = |r(\omega)|^2 = \frac{(n-1)^2 + K^2}{(n+1)^2 + K^2}$$

$$tg q = \frac{2K}{n^2 + K^2 - 1}$$

$$n = \frac{1 - R}{1 + R - 2R^{1/2} \cos q}$$

$$k = \frac{-2R^{1/2} \sin q}{1 + R - 2R^{1/2} \cos q}$$

If  $n$ ,  $K$  are known, we can get  $R$ ,  $\theta$ ; vice versa.

# Dielectric function

$$D(q, \omega) \equiv \epsilon(q, \omega) E(q, \omega)$$

$$\text{photon, } q \rightarrow 0, \epsilon = \epsilon(\omega, q \rightarrow 0) = \epsilon(\omega)$$

$$Q \sqrt{\epsilon(\omega)} = N(\omega)$$

$$\Rightarrow \epsilon(\omega) \equiv \epsilon_1(\omega) + i\epsilon_2(\omega) = (n(\omega) + iK(\omega))^2$$

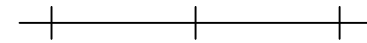
$$\epsilon_1(\omega) = n^2(\omega) - K^2(\omega)$$

$$\epsilon_2(\omega) = 2n(\omega) \cdot K(\omega)$$

or

$$n = \frac{1}{\sqrt{2}} \sqrt{\sqrt{\epsilon_1^2(\omega) + \epsilon_2^2(\omega)} + \epsilon_1(\omega)}$$

$$k = \frac{1}{\sqrt{2}} \sqrt{\sqrt{\epsilon_1^2(\omega) + \epsilon_2^2(\omega)} - \epsilon_1(\omega)}$$



0

$\pi/a \sim 1 \text{ \AA}^{-1}$

Infrared

$$q = 2\pi/\lambda \sim 10^{-4} \text{ \AA}^{-1}$$

# Conductivity

$$S = S_1(\omega) + S_2(\omega)$$

$$\text{By electrodynamics, } \epsilon(\omega) = 1 + \frac{4\pi i S(\omega)}{\omega}$$

In a solid, considering the contribution from ions or from high energy electronic excitations

$$\epsilon(\omega) = \epsilon_\infty + \frac{4\pi i S(\omega)}{\omega}$$

Now, we have several pairs of optical constants:

$$\left\{ \begin{array}{l} n(\omega), K(\omega) \\ R(\omega), \theta(\omega) \\ \varepsilon_1(\omega), \varepsilon_2(\omega) \\ \sigma_1(\omega), \sigma_2(\omega) \end{array} \right.$$

Usually,  $R(\omega)$  can be easily measured experimentally.



# Kramers-Kronig relation

-- the relation between the real and imaginary parts of a response function.

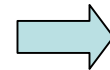
$$a_1(w) = \frac{2}{p} P \int_0^{+\infty} \frac{w' a_2(w') dw'}{w'^2 - w^2}$$

$$a_2(w) = \frac{-2w}{p} P \int_0^{\infty} \frac{a_1(w') dw'}{w'^2 - w^2}$$

For optical reflectance

$$r(w) = \sqrt{R(w)} e^{iq}$$

$$\Rightarrow \ln r(w) = (1/2) \ln R(w) + iq$$



$$q = \frac{w}{p} P \int_0^{\infty} \frac{\ln R(w')}{w^2 - w'^2} dw'$$

Low- $\omega$  extrapolations:

Insulator:  $R \sim \text{constant}$

Metal: Hagen-Rubens

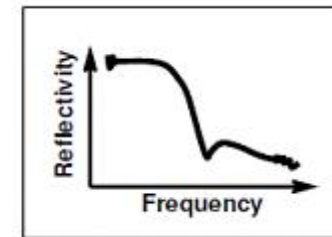
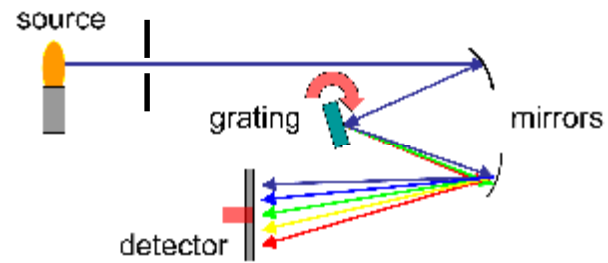
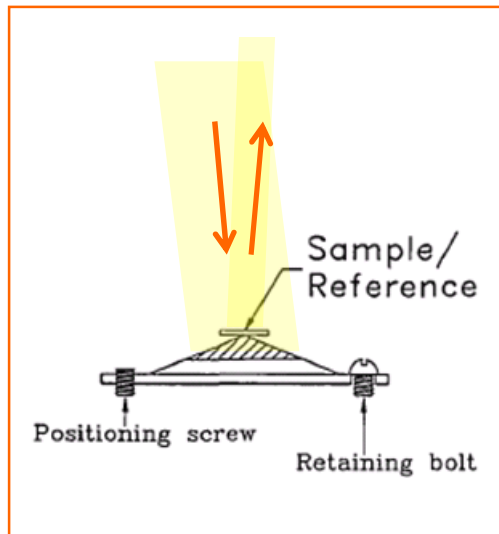
Superconductor: two-fluids model

High- $\omega$  extrapolations:

$R \sim \omega^p$  ( $p \sim 0.5-1$ , for intermediate region)

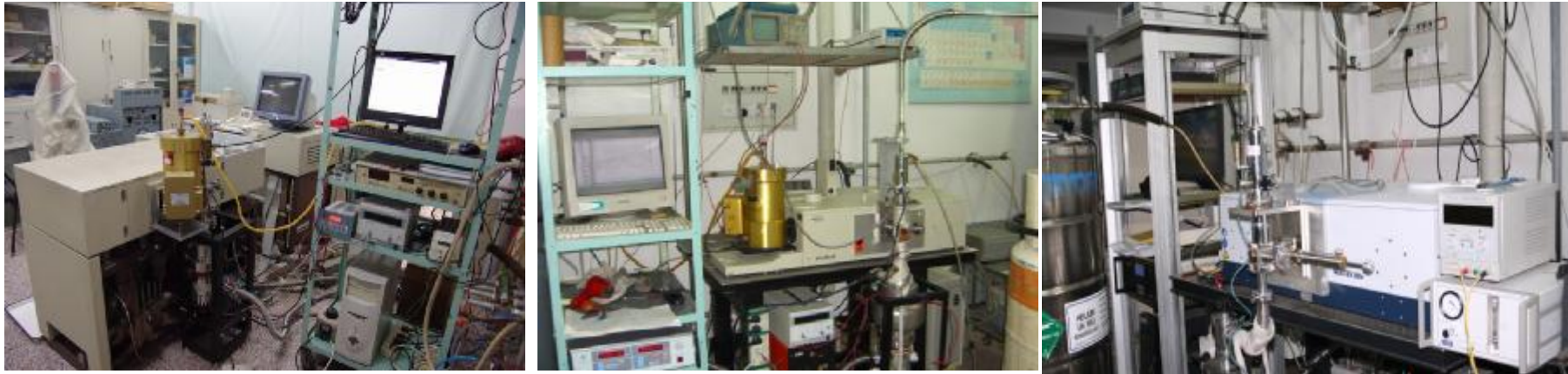
$R \sim \omega^{-n}$  ( $n=4$ , above interband transition)

# Reflectivity measurement



From  $R(\omega)$  to  $\sigma_1(\omega)$

$$R(\omega) \xrightarrow{\text{KK}} \theta(\omega) \rightarrow \begin{cases} n(\omega), \kappa(\omega) \\ \varepsilon_1(\omega), \varepsilon_2(\omega) \\ \sigma_1(\omega), \sigma_2(\omega) \end{cases}$$



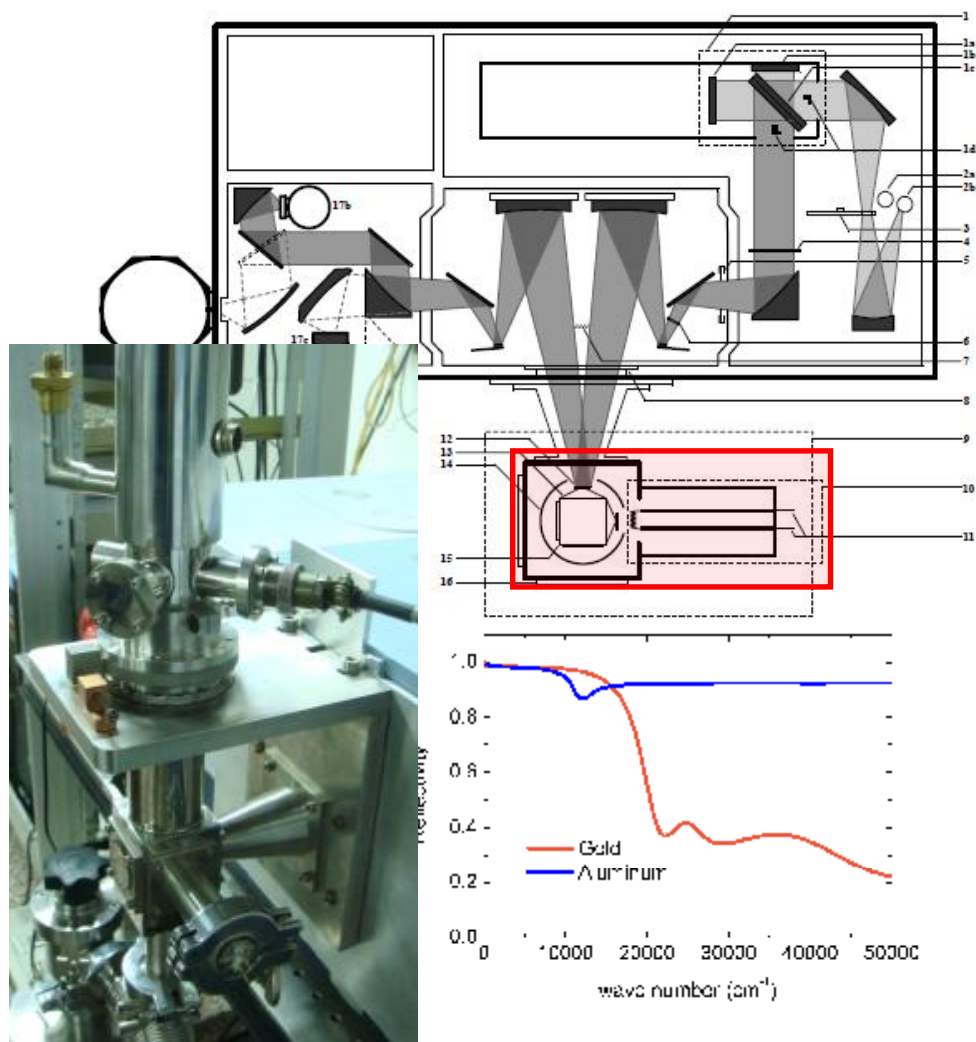
Si-beamsplitter for 113v

Bruker 113, 66v, 80v, and  
grating spectrometers

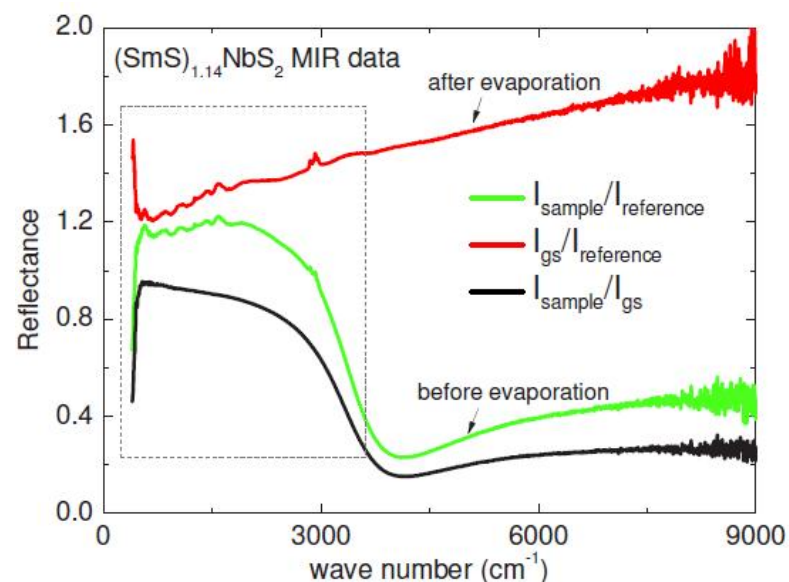
Energy range: 17 -50000  $\text{cm}^{-1}$  (2 meV~6 eV)

# In-situ overcoating technique

FT-IR spectrometer



*In situ* evaporation



$$\left(\frac{R_s}{R_r}\right)\left(\frac{R_{gs}}{R_r}\right)^{-1} \equiv \frac{R_s}{R_{gs}}$$

C. C. Homes *et al.*  
Applied Optics 32,2976(1993)



Fig. 5. Irregular piece broken from a crystal of SrTiO<sub>3</sub> used to measure the spectra in Fig. 6.

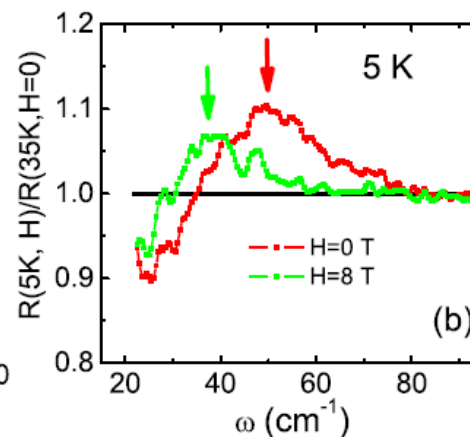
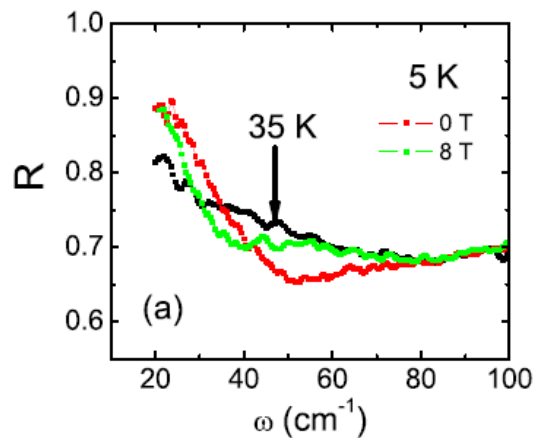
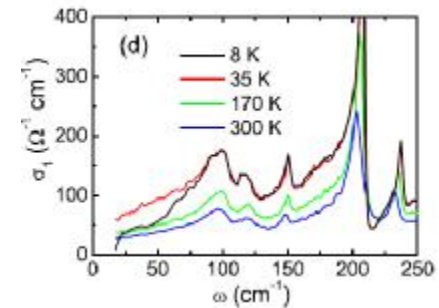
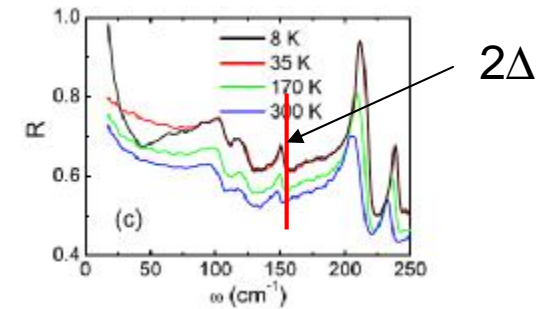


# Optical measurement under magnetic field

(10 Tesla split coils from Cryomagnetic Inc.)



$KxFe_{2-y}Se_2$   $T_c \sim 30$  K

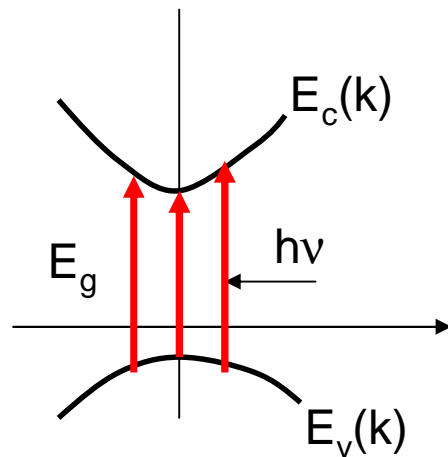


R. H. Yuan *et al.*,  
*Scientific Reports* 2,  
221 (2012)

# Interband transition

$$|v, k\rangle, E_v(k)$$

$$|c, k\rangle, E_c(k)$$



$$\hbar\omega = E_c(k) - E_v(k) \equiv E_{cv}(k)$$

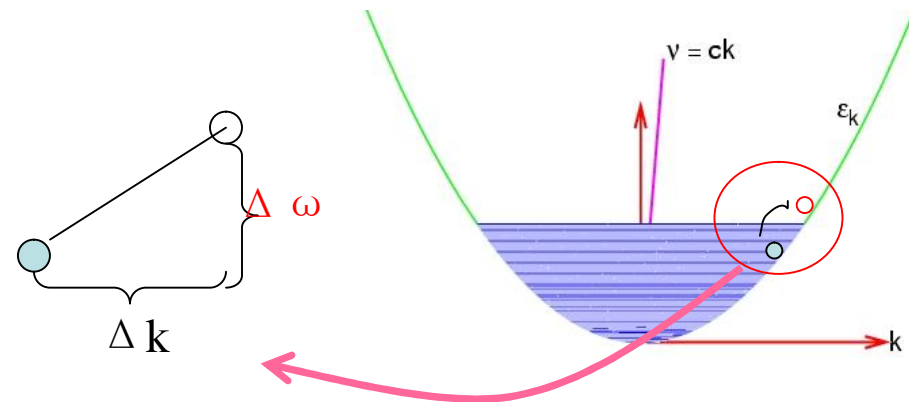
$$J(E) = \frac{V}{(2\pi)^3} \int \frac{ds}{|\nabla_k E_{cv}(k)|}$$

Kubo-Greenwood formula

$$e_2(\omega) = \frac{8\pi^2 e^2}{m^2 \omega^2} J(\hbar\omega) |\mathbf{r}_{vc}(\hbar\omega)|^2$$

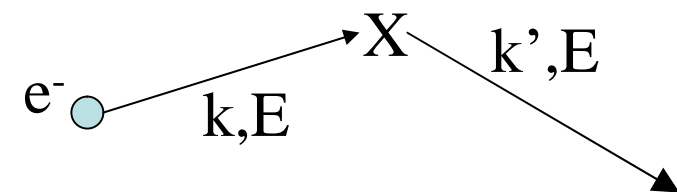
$$s_1(\omega) = \frac{1}{4\pi} \omega e_2(\omega)$$

# Intraband transition

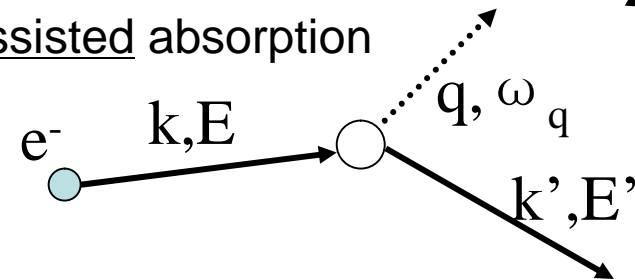


Infrared light **cannot be absorbed** directly by electron-hole excitation.

(a) Impurity-assisted absorption



(b) boson-assisted absorption



**Holstein process, if phonons are involved.**

# Drude model

$$S(w) = \frac{S_0}{1 - i\omega t} = \frac{w_p^2}{4\pi} \frac{1}{1/t - i\omega}$$

$$e(\omega) = e_\infty + \frac{4\pi i}{\omega} S(\omega)$$

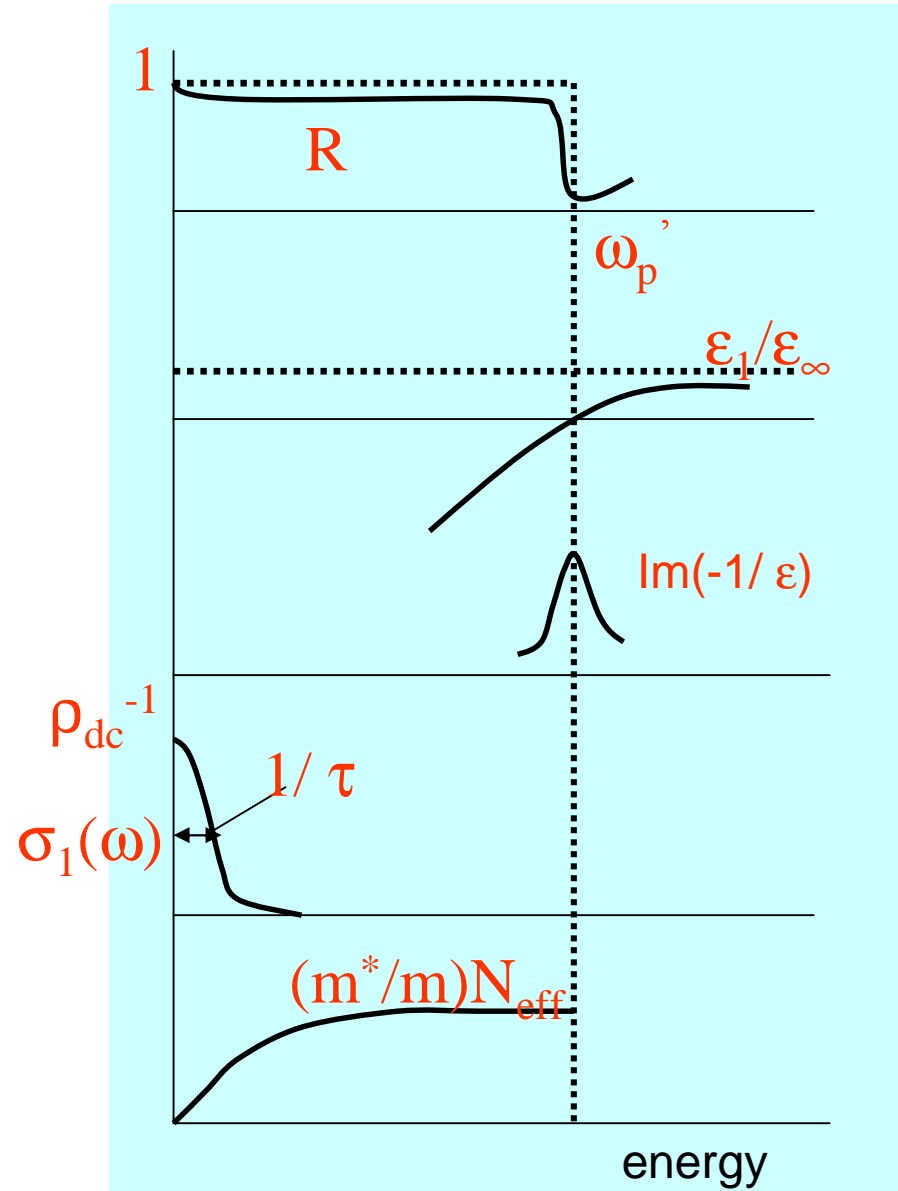
$$\Rightarrow e_1 = e_\infty - \frac{w_p^2}{\omega^2 + 1/t^2}$$

$$e_2 = \frac{4\pi S_1}{\omega} = \frac{w_p^2 t}{\omega} \frac{1}{1 + \omega^2 t^2}$$

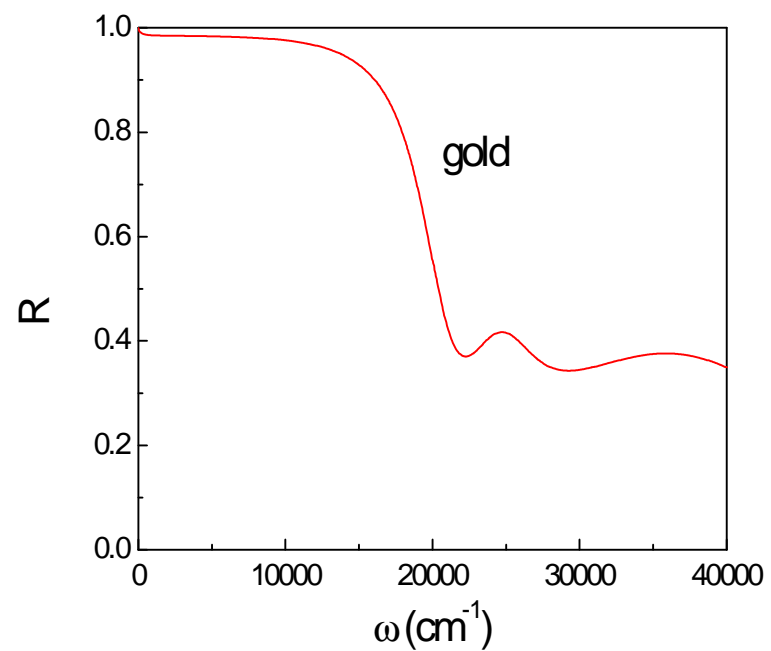
$$\text{Im}\left\{\frac{-1}{e(\omega)}\right\} = \frac{w_p^2 \omega / t}{(\omega^2 - w_p^2)^2 + \omega^2 t^{-2}}$$

$$w_p' = w_p / \sqrt{e_\infty}$$

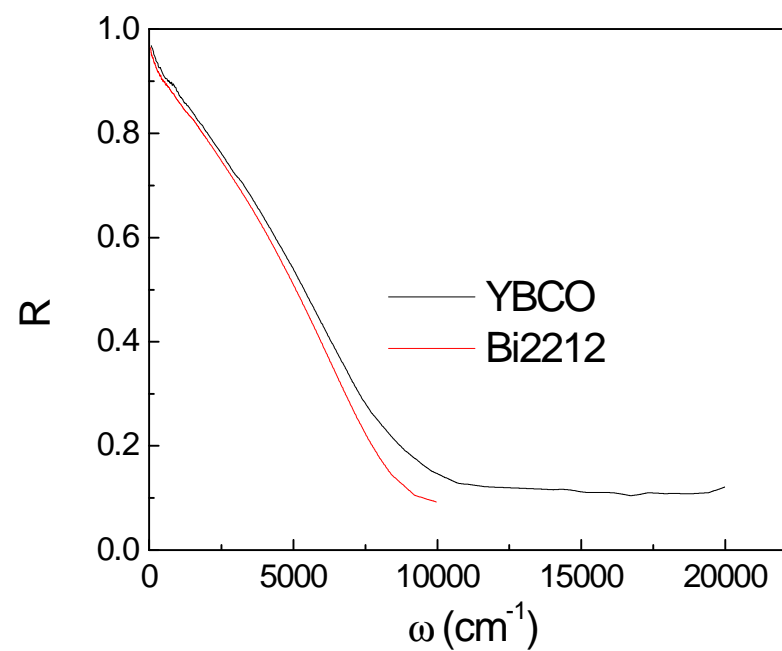
$$\int_0^\infty S_1(\omega) d\omega = \frac{w_p^2}{8}$$



## Simple metal

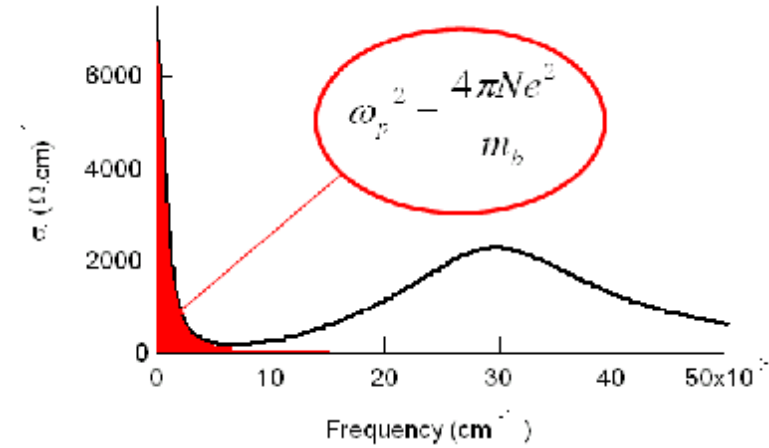


## High- $T_c$ cuprates





# Simple metal

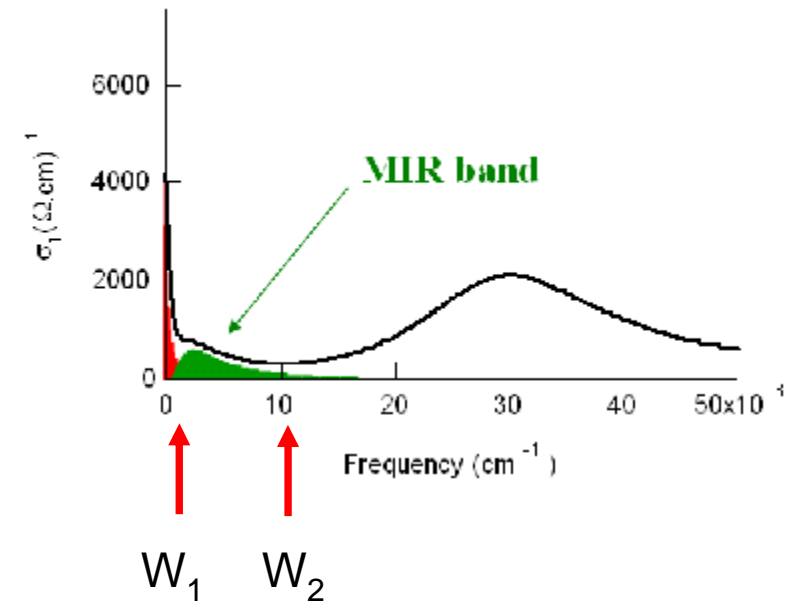


# Correlated metal

$$\omega_p^{\text{Drude}^2} = \frac{4\pi N e^2}{m^*}$$

$$\omega_p^{\text{Tot}^2} = \omega_p^{\text{Drude}^2} + \omega_p^{\text{MIR}^2} = \frac{4\pi N e^2}{m_b}$$

$$m^*/m_b = \frac{\omega_p^{\text{Tot}^2}}{\omega_p^{\text{Drude}^2}}$$



or

$$\frac{m^*}{m_B} = \frac{\int_0^{W_2} S_1(\omega, T > T_{co}) d\omega}{\int_0^{W_1} S_1(\omega, T \ll T_{co}) d\omega}$$

for heavy fermions

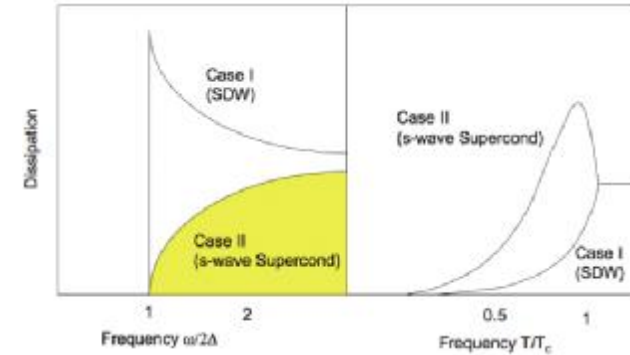
# Symmetry broken state

## Superconductor vs density wave state

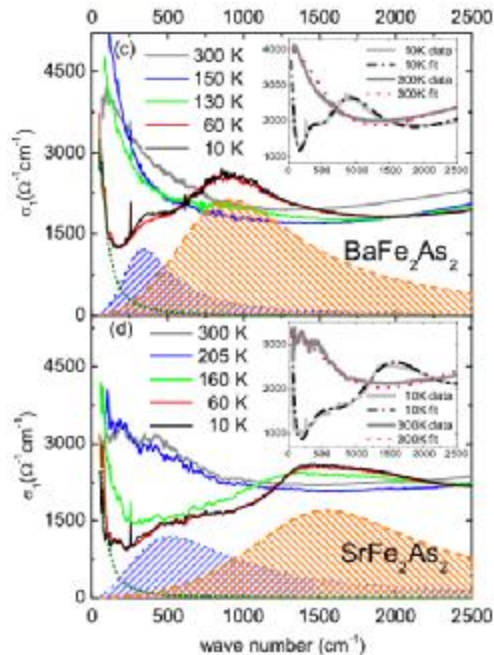
$$\frac{\sigma_1(\omega, T)}{\sigma_n} = \frac{2}{\hbar\omega} \int_{\Delta}^{\infty} \frac{[f(E) - f(E + \hbar\omega)](E^2 \pm \Delta^2 + \hbar\omega E)}{(E^2 - \Delta^2)^{1/2}[(E + \hbar\omega)^2 - \Delta^2]^{1/2}} dE$$

$$- \frac{1}{\hbar\omega} \int_{\Delta - \hbar\omega}^{-\Delta} \frac{[1 - 2f(E + \hbar\omega)](E^2 \pm \Delta^2 + \hbar\omega E)}{(E^2 - \Delta^2)^{1/2}[(E + \hbar\omega)^2 - \Delta^2]^{1/2}} dE,$$

- for case I  
+ for case II

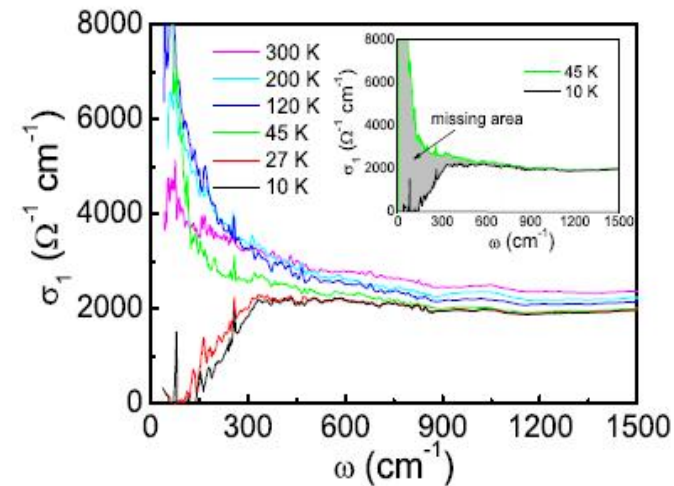


### AFe<sub>2</sub>As<sub>2</sub> (A=Ba, Sr), SDW gap



W.Z.Hu et al.  
PRL (08)

### Ba<sub>0.6</sub>K<sub>0.4</sub>Fe<sub>2</sub>As<sub>2</sub>, SC gap



G. Li et al. PRL (08)

URu<sub>2</sub>Si<sub>2</sub>

## Colloquium: Hidden order, superconductivity, and magnetism: The unsolved case of URu<sub>2</sub>Si<sub>2</sub>

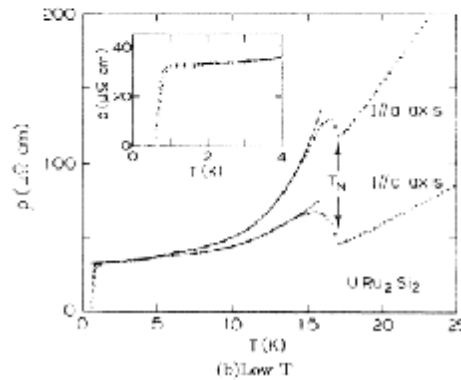
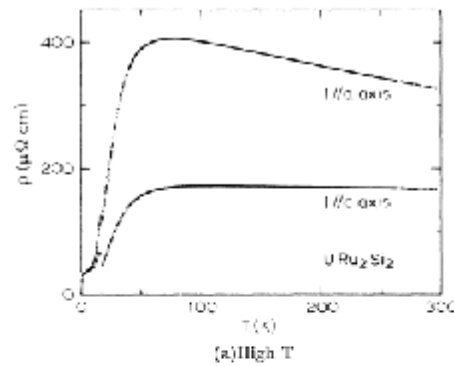
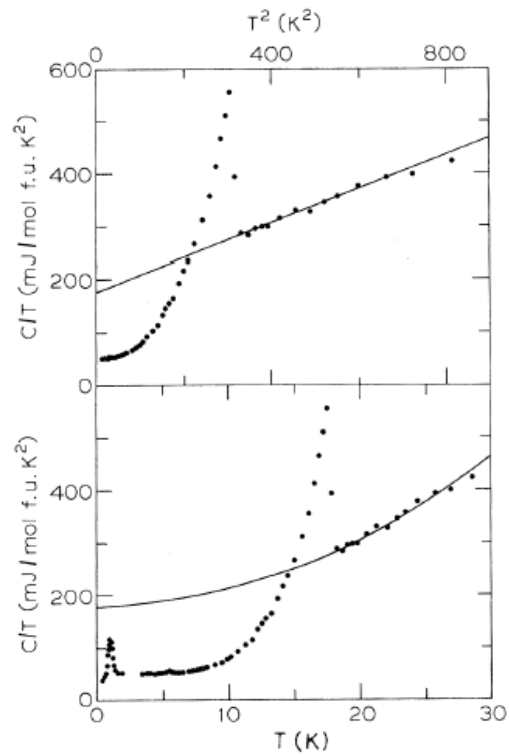
J. A. Mydosh\*

Kamerlingh Onnes Laboratory, Leiden University,  
P.O. Box 9504, NL-2300 RA Leiden, The Netherlands

P. M. Oppeneer†

Department of Physics and Astronomy, Uppsala University,  
P.O. Box 516, S-75120 Uppsala, Sweden

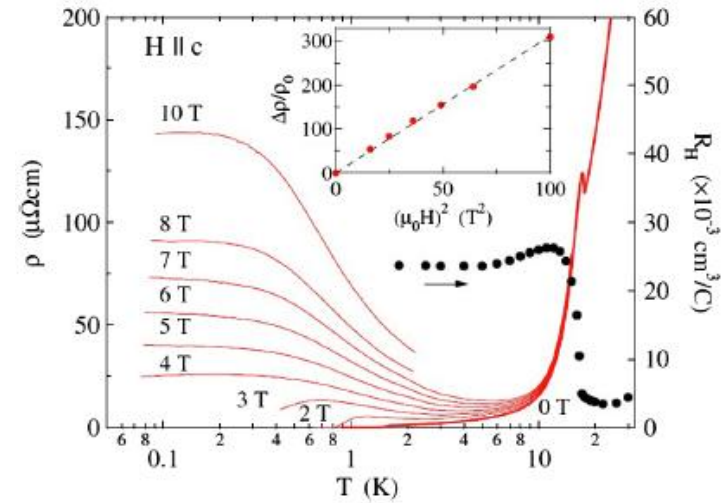
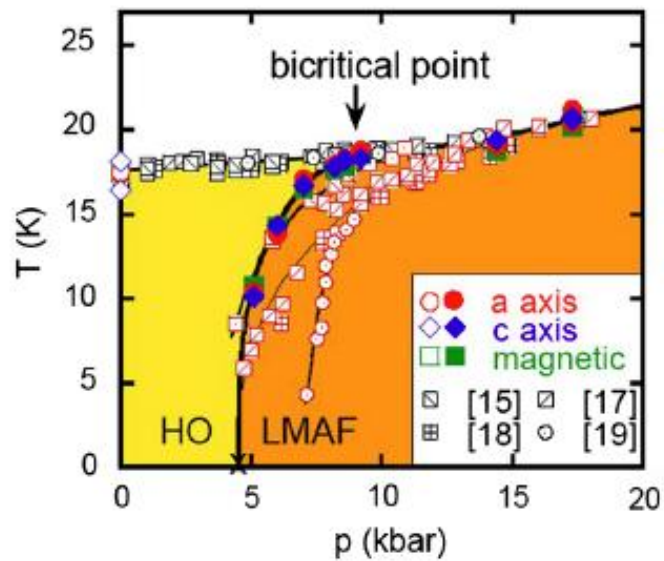
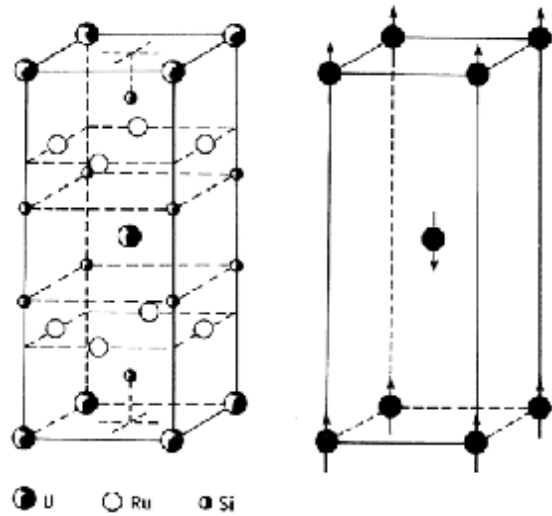
(published 16 November 2011)



- Ø Itinerant AFM
- Ø CDW/SDW
- Ø U-moment AFM

Palstra et al.

C. Broholm et al

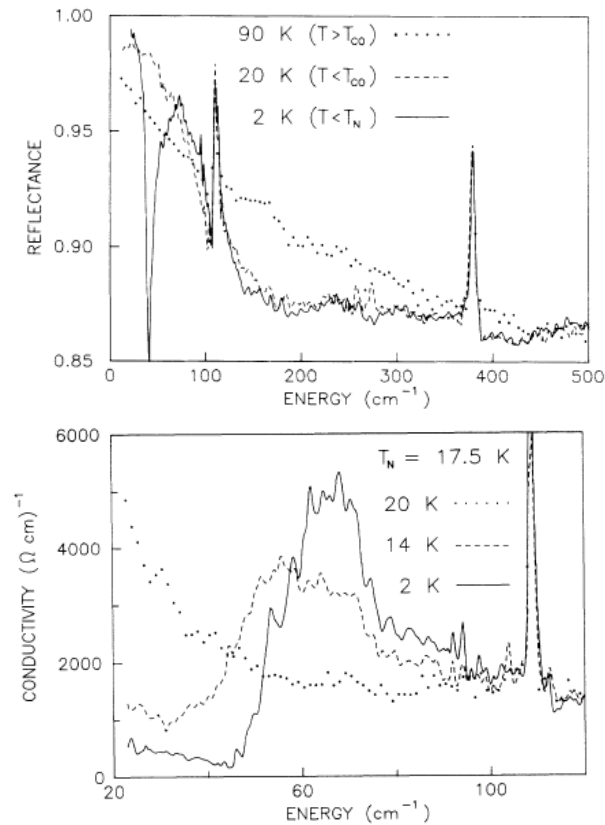


Kasahara et al.

Semimetal

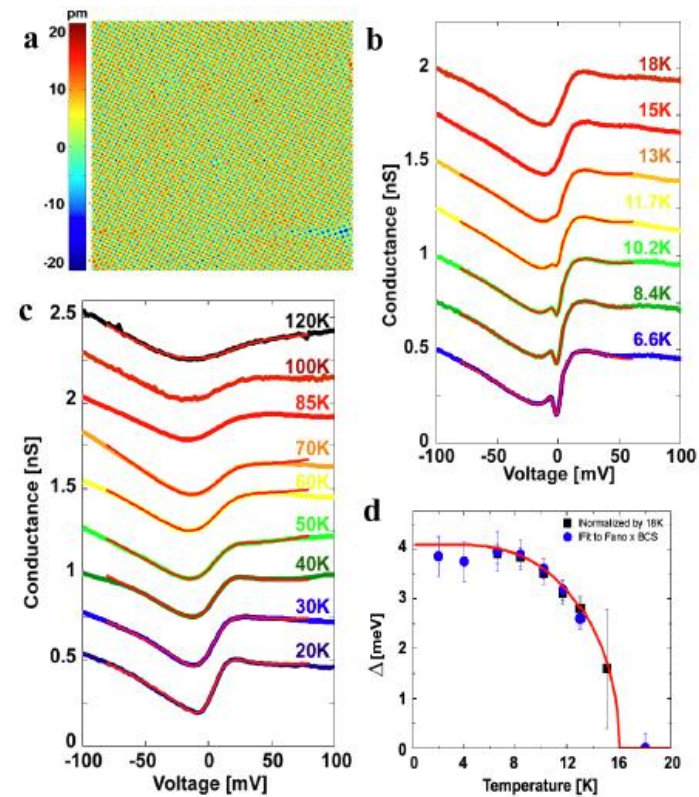
A number of experiments indicate gap opening below  $T_H$

Optical spectroscopy



Bonn et al. PRL 1988

STM

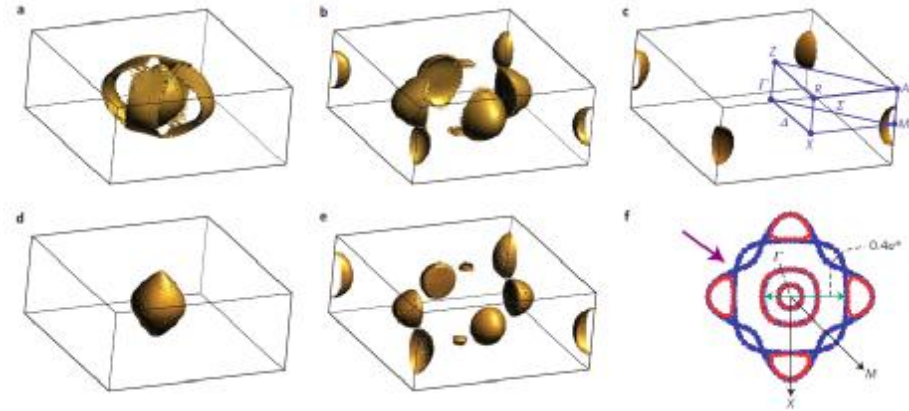
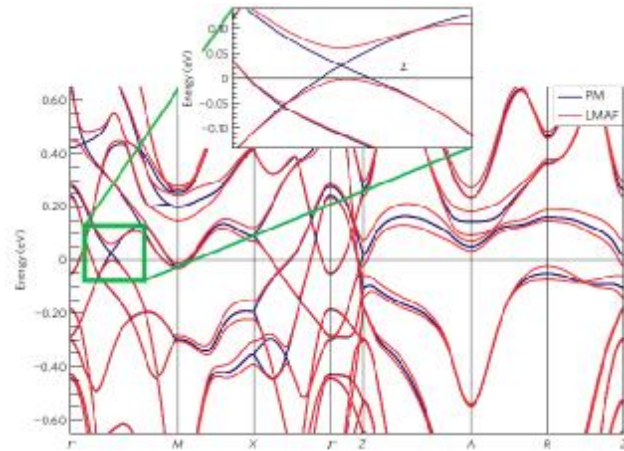


Aynajian et al, PNAS 2010

# Hidden order in URu<sub>2</sub>Si<sub>2</sub> originates from Fermi surface gapping induced by dynamic symmetry breaking

nature  
materials  
2009

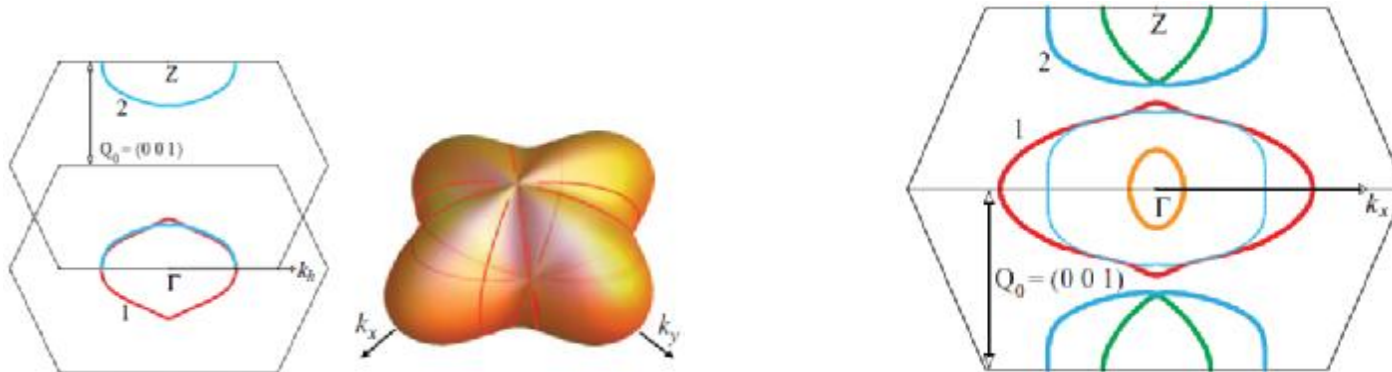
S. Elgazzar<sup>1\*</sup>, J. Ruzs<sup>1</sup>, M. Amft<sup>1</sup>, P. M. Oppeneer<sup>1†</sup> and J. A. Mydosh<sup>2</sup>



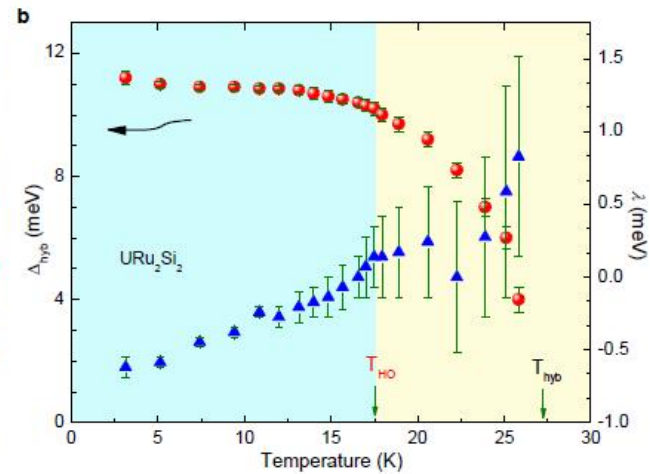
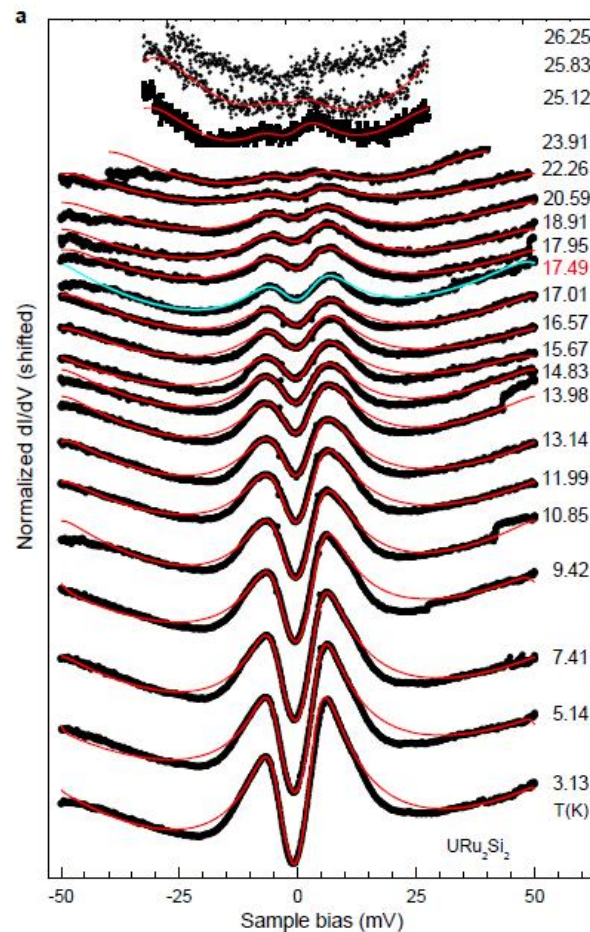
PHYSICAL REVIEW B **84**, 241102(R) (2011)

## Spin and orbital hybridization at specifically nested Fermi surfaces in URu<sub>2</sub>Si<sub>2</sub>

P. M. Oppeneer,<sup>1</sup> S. Elgazzar,<sup>2</sup> J. Ruzs,<sup>1</sup> Q. Feng,<sup>1</sup> T. Durakiewicz,<sup>3</sup> and J. A. Mydosh<sup>4</sup>



However, some other experiments indicate gap formation up to a higher  $T \sim 25 - 30$  K



Point contact tunneling spectroscopy

WK Park et al. arXiv:1110.5541



## Evidence of a hidden-order pseudogap state in URu<sub>2</sub>Si<sub>2</sub> using ultrafast optical spectroscopy

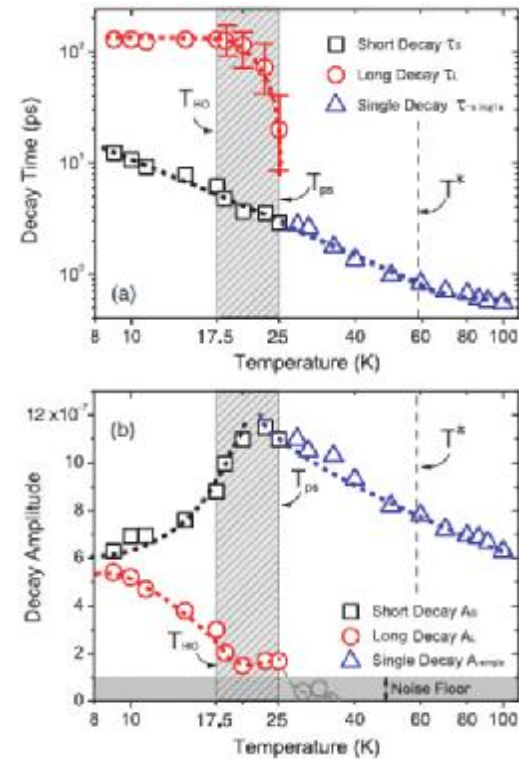
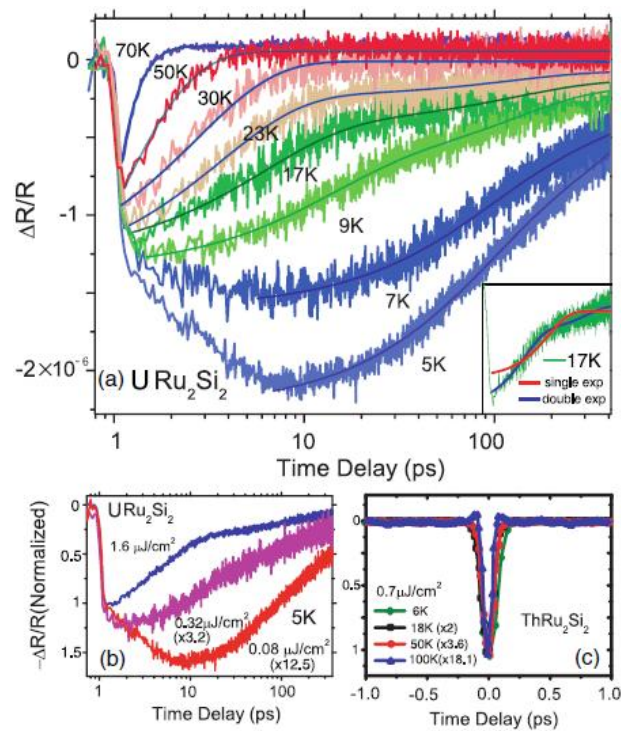
M. K. Liu and R. D. Averitt\*

*Department of Physics, Boston University, 590 Commonwealth Avenue, Boston, Massachusetts 02215, USA*

T. Durakiewicz, P. H. Tobash, E. D. Bauer, S. A. Trugman, A. J. Taylor, and D. A. Yarotski†

*Los Alamos National Laboratory, Los Alamos, New Mexico 87545, USA*

(Received 26 July 2011; revised manuscript received 20 September 2011; published 11 October 2011)

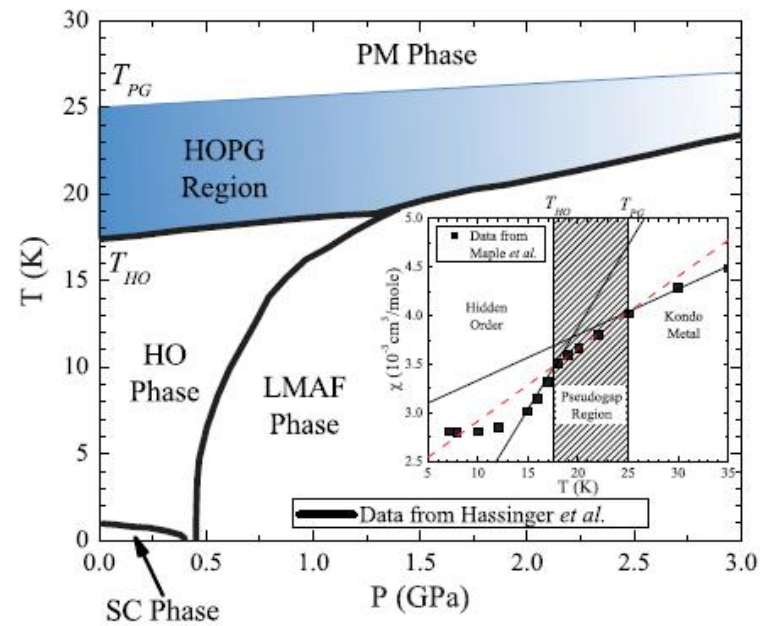


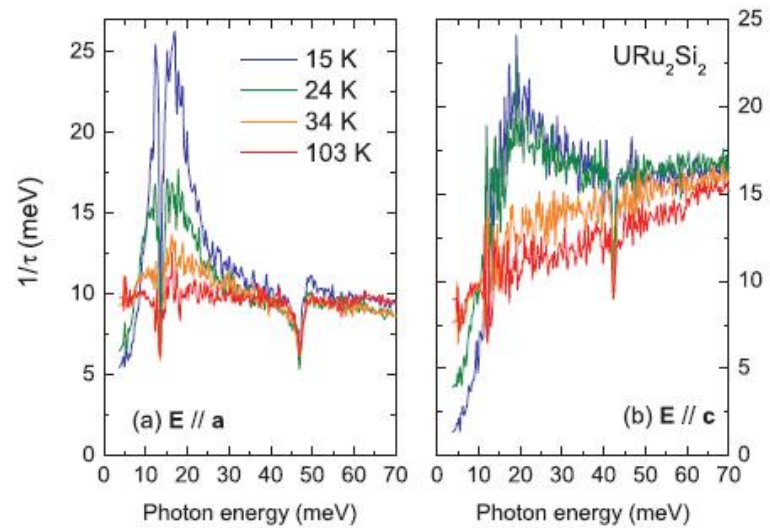
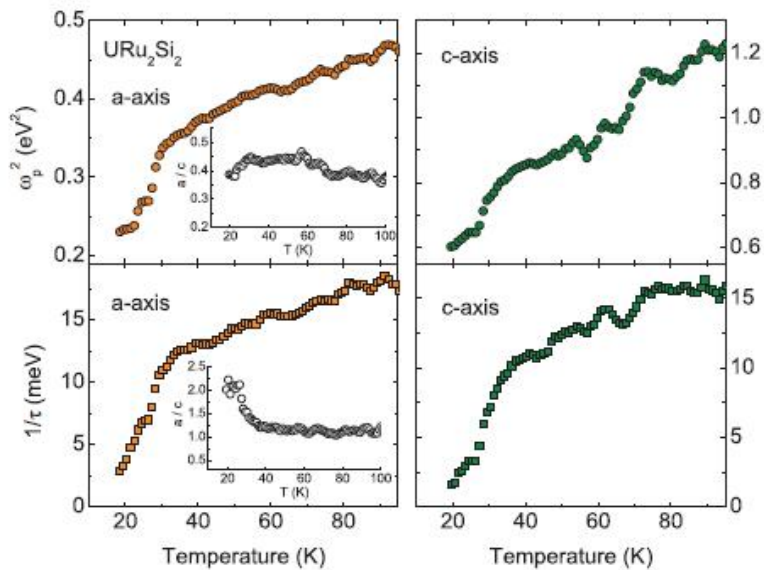
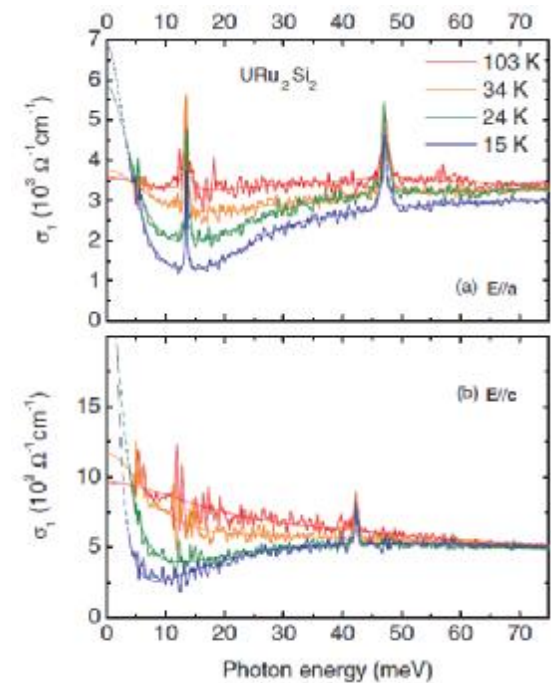
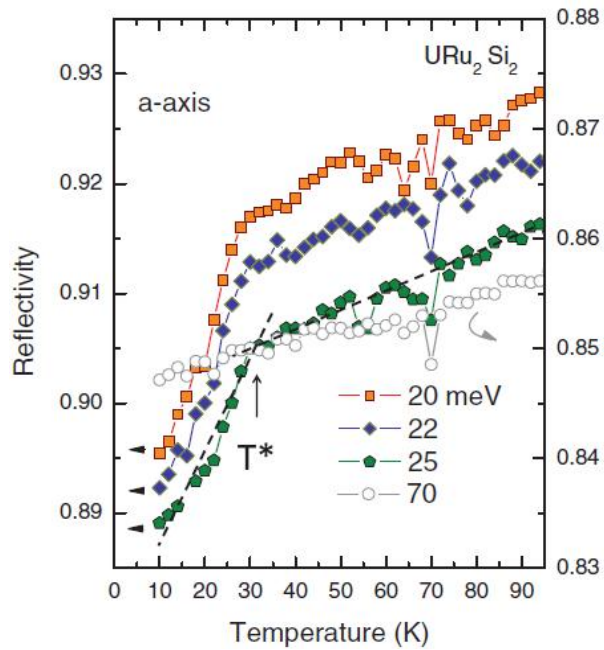
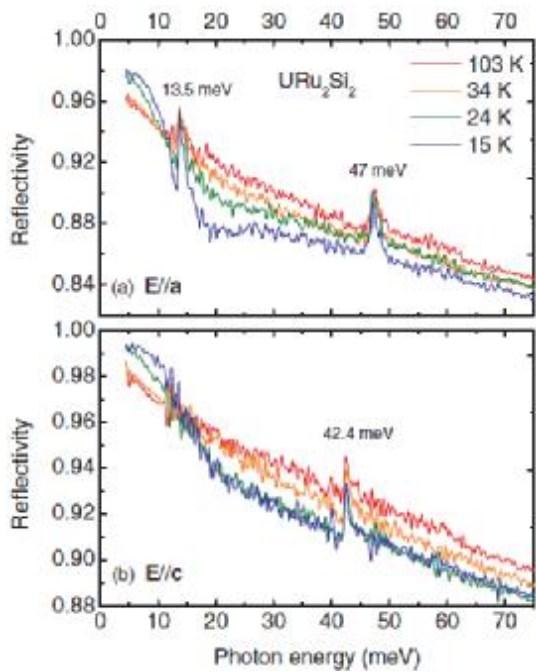
A gap would impede the relaxation of excited quasiparticles.

$$\Delta R(t)/R = A_0 + A_S \exp(-t/\tau_S) + A_L \exp(-t/\tau_L), \text{ where } \tau_S \text{ and } \tau_L \text{ are the short and long decay times, respectively.}$$

## Hidden-order pseudogap in URu<sub>2</sub>Si<sub>2</sub>

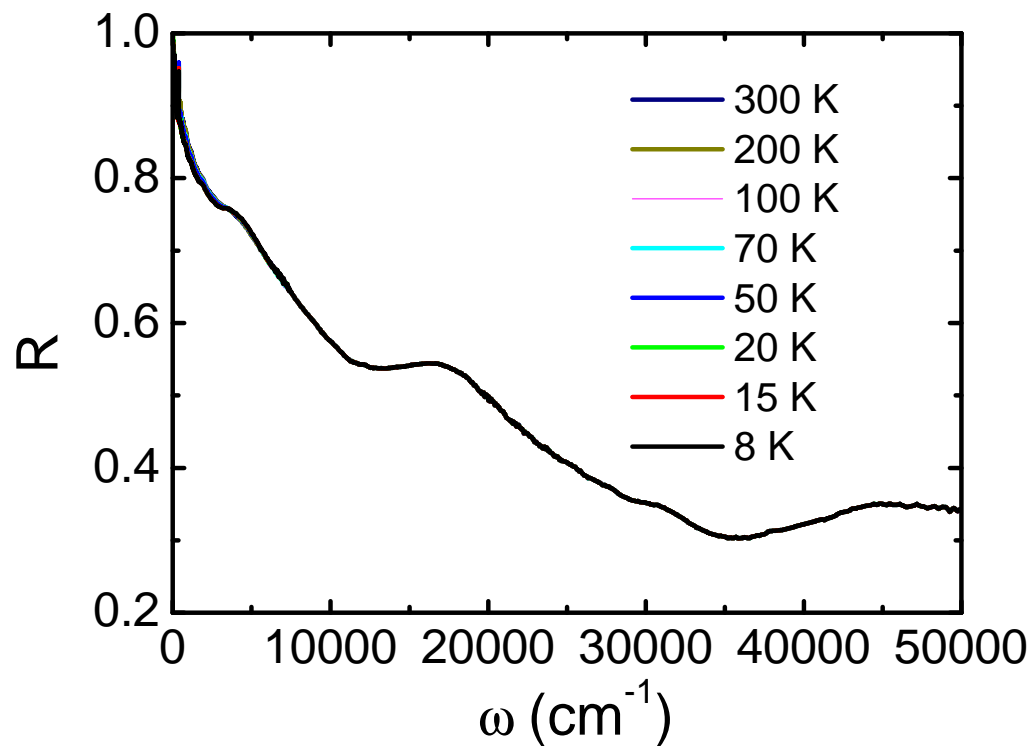
J. T. Haraldsen,<sup>1,2</sup> Y. Dubi,<sup>3</sup> N. J. Curro,<sup>4</sup> and A. V. Balatsky<sup>1,2</sup>



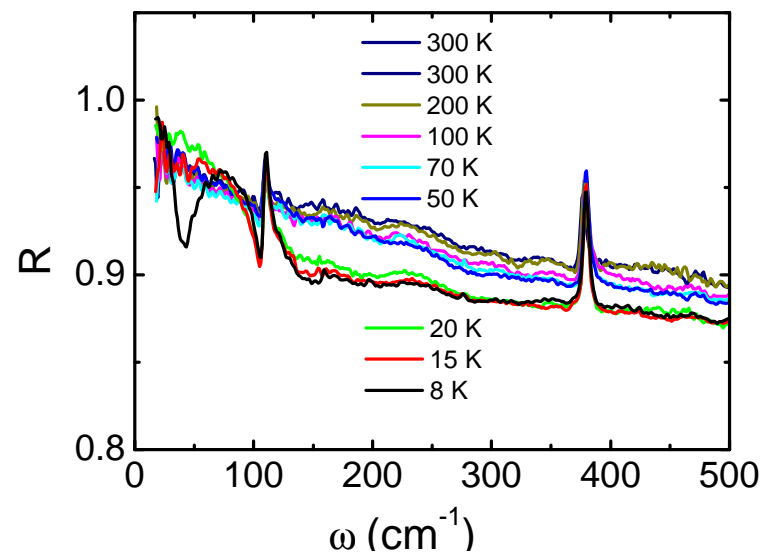
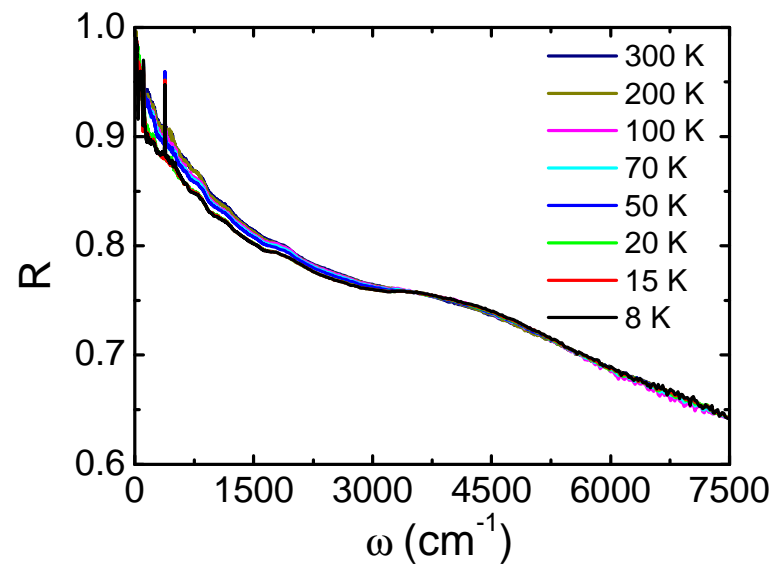


J. Levallois et al PRB 2011

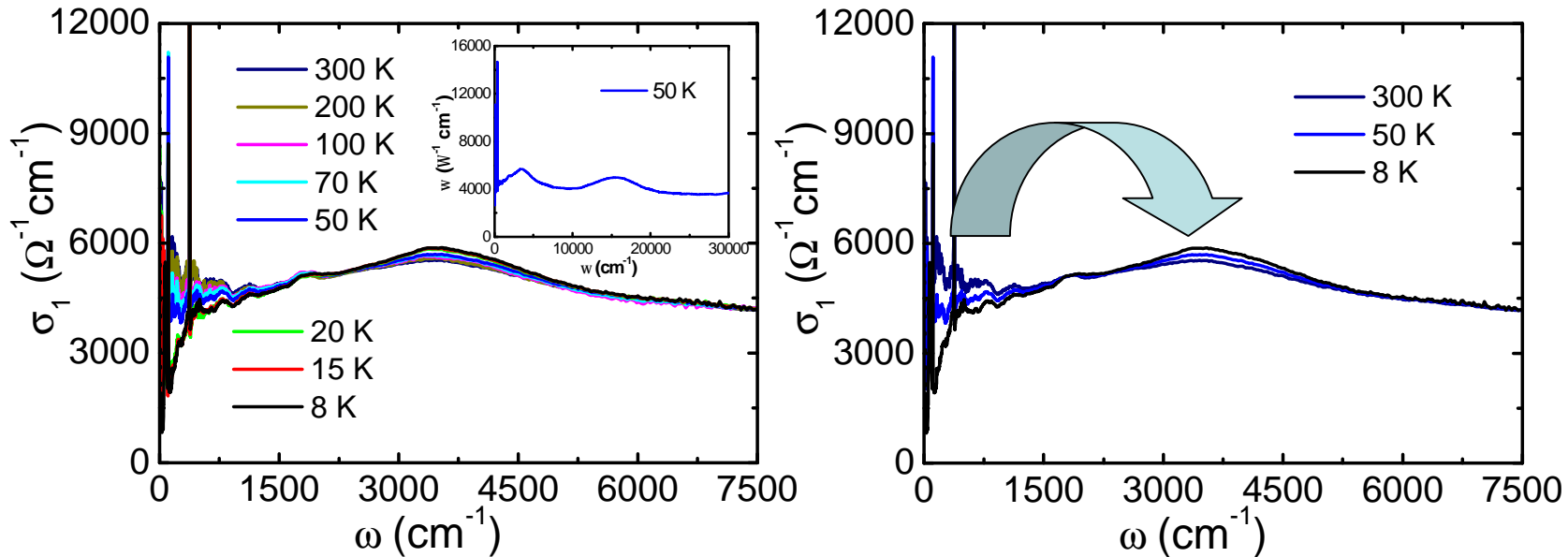
# Reflectance



Samples from G. Luke

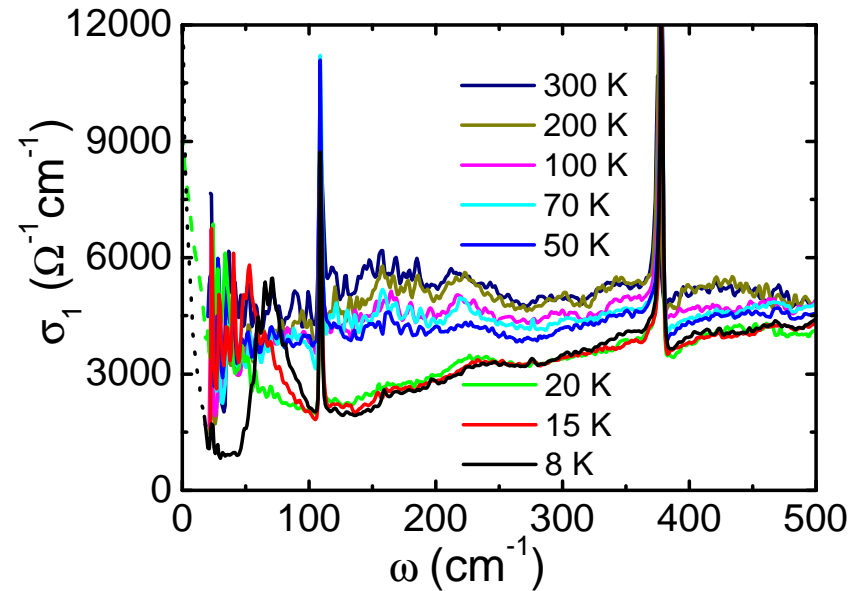
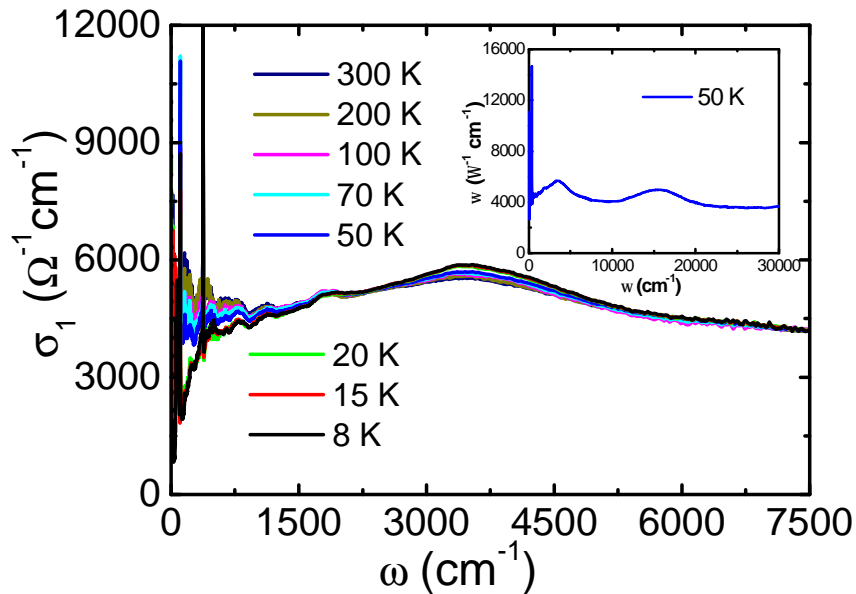


# Optical conductivity



For  $T > 50$  K,  $\sigma_1(\omega)$  shows a non-metallic behavior. The Drude component is completely absent. Actually,  $\sigma_1(\omega)$  shows a decreasing tendency with decreasing  $\omega$ . Clearly, there are no well defined quasiparticles above 50 K.

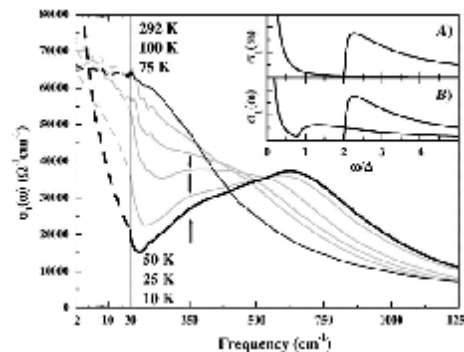
With  $T$  from 300 K to 50 K, the spectral weight is transferred from the low- $\omega$  regime (below 2000  $\text{cm}^{-1}$ ) to higher  $\omega$  region (centered at about 4000  $\text{cm}^{-1}$ ).



∅  $T \ll T_{co}$ , roughly below 20 K, there appears an abrupt spectral weight suppression below 400  $cm^{-1}$ .  $\rightarrow$  formation of hybridization gap.

∅ A small part of the suppressed spectral weight was transferred to the low- $\omega$  side, leading to a narrow Drude component, while the majority of the suppressed spectral weight was still transferred to the high  $\omega$  side centered near 4000  $cm^{-1}$ .

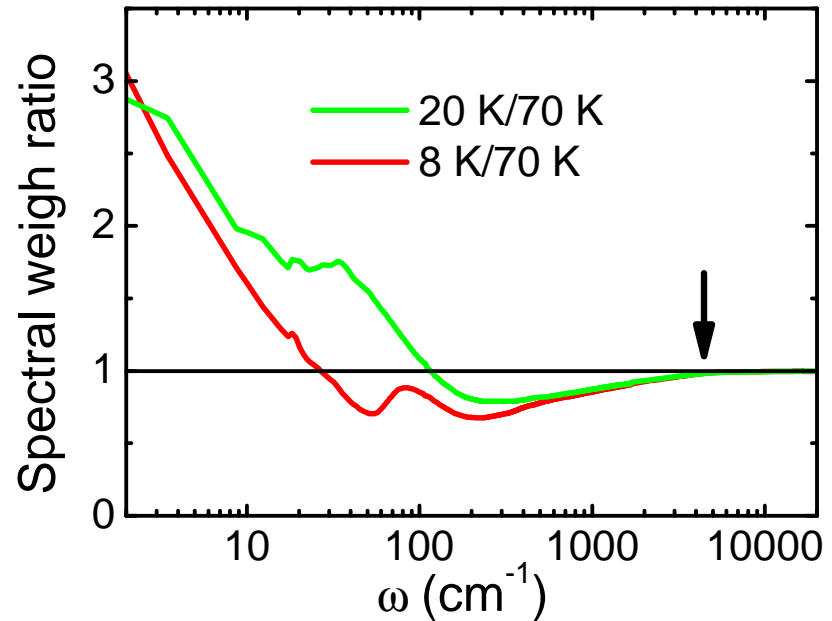
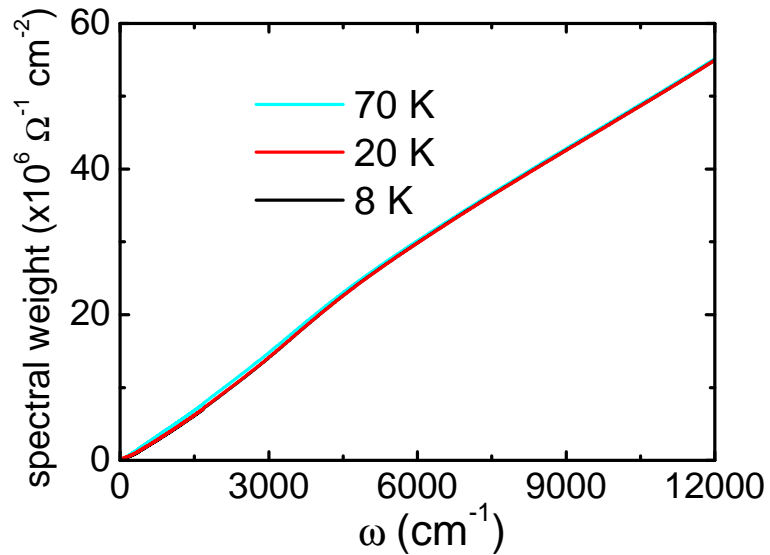
This energy scale of the spectral weight transfer is high compared to some 4f electron-based heavy fermion systems, e.g. CeCoIn5.



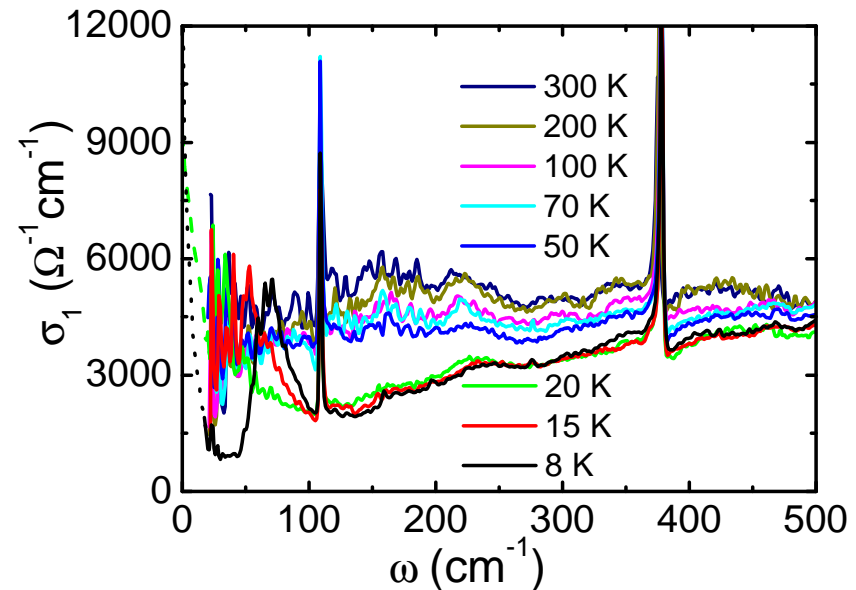
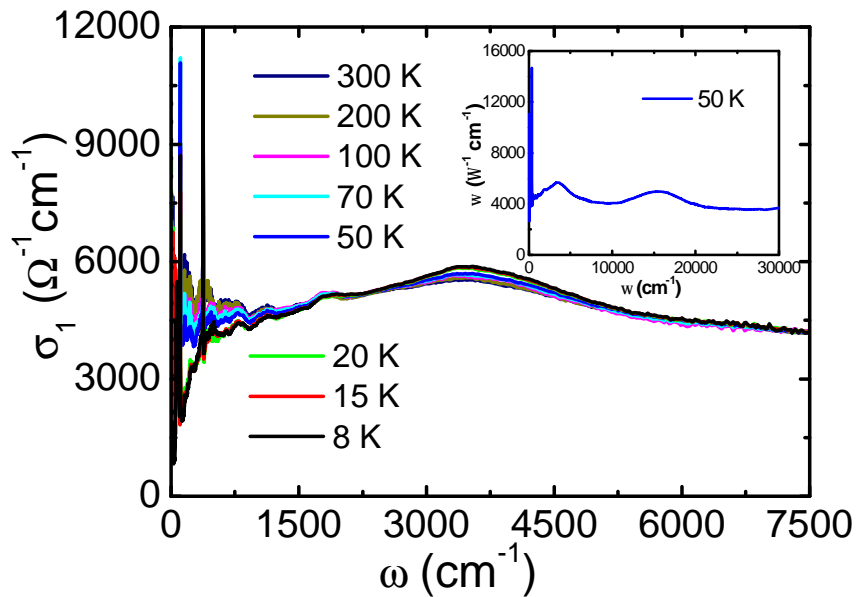
CeCoIn5

Singley, et al.  
PRB 2002

# Spectral weight transfer

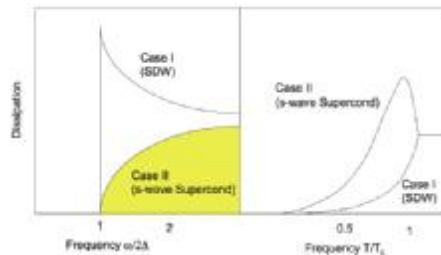


$$w_p^2 \propto \int_0^w s_1(w) dw \quad \left\{ \begin{array}{l} w_p = 1.95 \times 10^4 \text{ cm}^{-1} \\ w_p = 4.28 \times 10^3 \text{ cm}^{-1} \\ w_p = 2.094 \times 10^3 \text{ cm}^{-1} \end{array} \right. \quad \begin{array}{l} W=2000 \text{ cm}^{-1} \text{ for } T=50 \text{ K and } 300 \text{ K;} \\ W=135 \text{ cm}^{-1} \text{ for } T=20 \text{ K} \\ W=42 \text{ cm}^{-1} \text{ for } T=8 \text{ K} \end{array}$$



Ø The formation of hybridization gap is associated with renormalization of heavy quasiparticle. The mass enhancement is roughly  $m^*/m_B \sim 21$ .

Ø Below the  $T_H$ , we observe clearly the opening of a density-wave type energy gap: a large fraction of the coherent Drude spectral weight was removed and piled up just above the energy gap of  $60 \text{ cm}^{-1}$  ( $2\Delta/k_B T_c \sim 5.7$ ).  $n_{8K}/n_{20K} \sim 0.24$ .



“Text book”-like density wave type energy gap below  $T_H$ .



## Conclusions:

∅ different from the point contact tunneling spectroscopy measurement, the Hybridization gap ( $\sim 15$  meV) is completely different from the density-wave type gap ( $2\Delta \sim 8$  eV) in the hidden order state;

∅ No other pseudogap is detected;

∅ The formation of the hybridization gap is a crossover phenomenon, being associated with the formation of a narrow Drude component (or well-defined heavy quasiparticles);

∅ The opening of the density wave gap below  $T_H$  results in the removal of a large fraction of Fermi surfaces (about 75%) and a rapid reduction of the scatterings.

**Thank you!**

Hubbard U physics:

$\rho(\omega)$

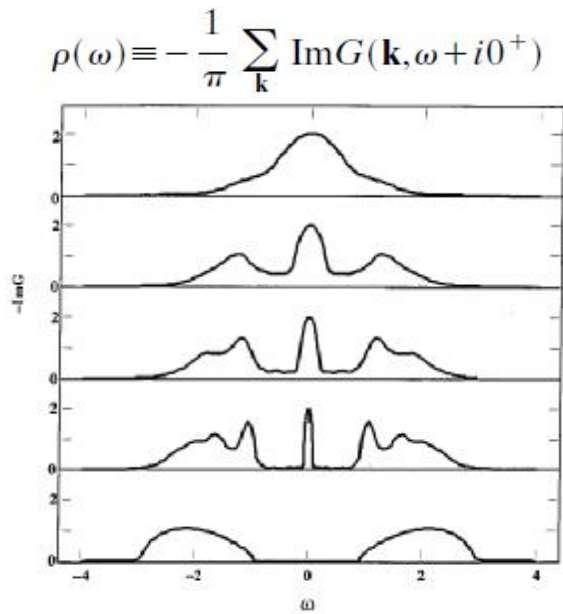
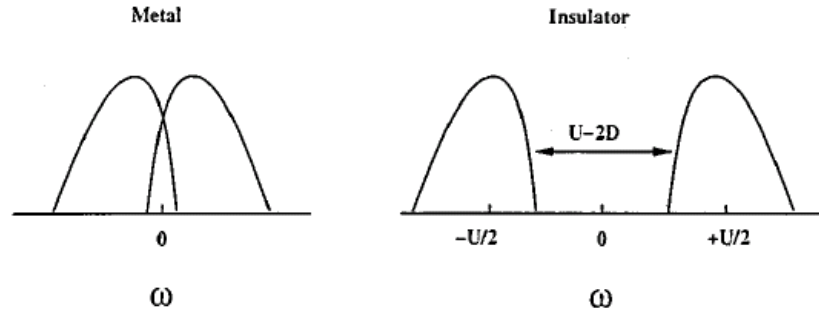
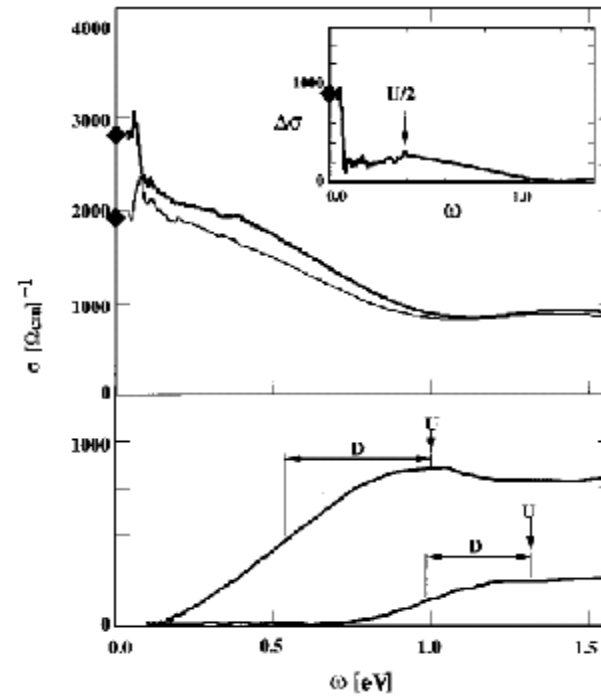


FIG. 30. Local spectral density  $\pi D\rho(\omega)$  at  $T=0$ , for several values of  $U$ , obtained by the iterated perturbation theory approximation. The first four curves (from top to bottom,  $U/D = 1, 2, 2.5, 3$ ) correspond to an increasingly correlated metal, while the bottom one ( $U/D=4$ ) is an insulator.



V2O3

served. As  $T$  is lowered, there is an enhancement of the spectrum at intermediate frequencies of order 0.5 eV; more notably, a sharp low-frequency feature emerges that extends from 0 to 0.15 eV.

DFMT